Selective filling of photonic crystal fibers using focused ion beam milled microchannels

Wang, Fei; Yuan, Scott Wu; Hansen, Ole; Bang, Ole

Published in:
Optics Express

Link to article, DOI:
10.1364/OE.19.017585

Publication date:
2011

Document Version
Publisher's PDF, also known as Version of record

Selective filling of photonic crystal fibers using focused ion beam milled microchannels

Fei Wang,[1,4] Wu Yuan,[2,*] Ole Hansen[1,3] and Ole Bang[2]

[1]*Dept. of Micro- and Nanotechnology, Technical University of Denmark, DK-2800 Kgs. Lyngby, Denmark*
[2]*Dept. of Photonics Engineering, Technical University of Denmark, DK-2800 Kgs. Lyngby, Denmark*
[3]*CINF, Technical University of Denmark, DK-2800 Kgs. Lyngby, Denmark*
[4]*Fei.Wang@nanotech.dtu.dk*
**Scottwyuan@gmail.com*

Abstract: We introduce a versatile, robust, and integrated technique to selectively fill fluid into a desired pattern of air holes in a photonic crystal fiber (PCF). Focused ion beam (FIB) is used to efficiently mill a microchannel on the end facet of a PCF before it is spliced to a single-mode fiber (SMF). Selected air holes are therefore exposed to the atmosphere through the microchannel for fluid filling. A low-loss in-line tunable optical hybrid fiber device is demonstrated by using such a technique.

OCIS codes: (060.4005) Microstructured fibers; (060.2310) Fiber optics; (060.2280) Fiber design and fabrication; (230.1150) All-optical devices.

References and links

1. T. Larsen, A. Bjarklev, D. Hermann, and J. Broeng, "Optical devices based on liquid crystal photonic bandgap fibres," Opt. Express **11**(20), 2589–2596 (2003), http://www.opticsexpress.org/abstract.cfm?URI=oe-11-20-2589.
2. W. Yuan, L. Wei, T. T. Alkeskjold, A. Bjarklev, and O. Bang, "Thermal tunability of photonic bandgaps in liquid crystal infiltrated microstructured polymer optical fibers," Opt. Express **17**(22), 19356–19364 (2009), http://www.opticsexpress.org/abstract.cfm?URI=oe-17-22-19356.
3. D. K. C. Wu, B. T. Kuhlmey, and B. J. Eggleton, "Ultrasensitive photonic crystal fiber refractive index sensor," Opt. Lett. **34**(3), 322–324 (2009).
4. F. Benabid, F. Couny, J. C. Knight, T. A. Birks, and P. S. Russell, "Compact, stable and efficient all-fibre gas cells using hollow-core photonic crystal fibres," Nature **434**(7032), 488–491 (2005).
5. B. Eggleton, C. Kerbage, P. Westbrook, R. Windeler, and A. Hale, "Microstructured optical fiber devices," Opt. Express **9**(13), 698–713 (2001), http://www.opticsexpress.org/abstract.cfm?URI=oe-9-13-698.
6. C. R. Rosberg, F. H. Bennet, D. N. Neshev, P. D. Rasmussen, O. Bang, W. Krolikowski, A. Bjarklev, and Y. S. Kivshar, "Tunable diffraction and self-defocusing in liquid-filled photonic crystal fibers," Opt. Express **15**(19), 12145–12150 (2007), http://www.opticsexpress.org/abstract.cfm?URI=oe-15-19-12145.
7. L. Xiao, W. Jin, M. Demokan, H. Ho, Y. Hoo, and C. Zhao, "Fabrication of selective injection microstructured optical fibers with a conventional fusion splicer," Opt. Express **13**(22), 9014–9022 (2005), http://www.opticsexpress.org/abstract.cfm?URI=oe-13-22-9014.
8. Y. Huang, Y. Xu, and A. Yariv, "Fabrication of functional microstructured optical fibers through a selective-filling technique," Appl. Phys. Lett. **85**(22), 5182–5184 (2004).
9. Y. Wang, S. Liu, X. Tan, and W. Jin, "Selective-fluid-filling technique of microstructured optical fibers," J. Lightwave Technol. **28**, 3193–3196 (2010).
10. C. Martelli, P. Olivero, J. Canning, N. Groothoff, B. Gibson, and S. Huntington, "Micromachining structured optical fibers using focused ion beam milling," Opt. Lett. **32**(11), 1575–1577 (2007).
11. W. Yuan, F. Wang, A. Savenko, D. H. Petersen, and O. Bang, "Note: Optical fiber milled by focused ion beam and its application for Fabry-Pérot refractive index sensor," Rev. Sci. Instrum. **82**(7), 076103 (2011).
12. C. Martelli, P. Olivero, J. Canning, N. Groothoff, S. Prawer, S. Huntington, and B. Gibson, "Micromachining long period gratings in optical fibres using focussed ion beam," OSA Topical Meeting: Bragg Gratings, Photosensitivity and Poling (BGPP 2007), Quebec City, Canada, (2007).
13. S. Kang, H.-E. Joe, J. Kim, Y. Jeong, B.-K. Min, and K. Oh, "Subwavelength plasmonic lens patterned on a composite optical fiber facet for quasi-one-dimensional Bessel beam generation," Appl. Phys. Lett. **98**(24), 241103 (2011).
14. A. Cerqueira S, Jr., F. Luan, C. M. Cordeiro, A. K. George, and J. C. Knight, "Hybrid photonic crystal fiber," Opt. Express **14**(2), 926–931 (2006), http://www.opticsexpress.org/abstract.cfm?URI=oe-14-2-926.
15. A. Abeeluck, N. Litchinitser, C. Headley, and B. Eggleton, "Analysis of spectral characteristics of photonic bandgap waveguides," Opt. Express **10**(23), 1320–1333 (2002).
16. T. T. Alkeskjold, J. Laegsgaard, A. Bjarklev, D. S. Hermann, J. Broeng, J. Li, S. Gauza, and S. T. Wu, "Highly tunable large-core single-mode liquid-crystal photonic bandgap fiber," Appl. Opt. **45**(10), 2261–2264 (2006).

#152186 - $15.00 USD Received 1 Aug 2011; accepted 18 Aug 2011; published 22 Aug 2011

1. Introduction

Infiltration of functional materials, such as liquids [1–3], gas [4], and polymer [5], into the air holes of solid-core or hollow-core PCFs has attracted significant interest for the development of advanced passive or active optical fiber devices for communication and sensor applications. Selective filling of the holes of a PCF was, e.g., used to achieve asymmetric coupling [3], birefringence [5], hybrid guiding [5], tunable beam diffraction and self-defocusing [6], and high nonlinearity [4]. Various techniques have been used to achieve selective filling, such as collapsing air-holes with a fusion splicer [7], injection-cleaving exploiting the different filling speeds of holes of different sizes [8], direct manual gluing with a UV curable polymer [3], and micromachining with a femtosecond laser [9]. While the first two techniques can only be used for a limited number of specific hole configurations, direct gluing and femtosecond laser micromachining potentially allow the creation of arbitrary patterns of filled and unfilled holes. However, gluing holes manually and micromachining holes one by one with a femtosecond laser could be very time consuming and imprecise. Furthermore, the use of glue and the infiltration of functional materials in advance will make the subsequent splicing difficult. Most of the glue and functional materials cannot withstand the high temperature of fusion splicing and it will cause potential contamination to the splicer. To avoid the splicing problem, more advanced methods have been developed recently to carve a side access fan-shaped groove with a femtosecond laser [9] or a side access hole with FIB [10] in the PCF to expose the internal holes for material filling. With these methods, only a limited number of infiltration patterns can be realized. Although FIB is a versatile tool, it is not easy to accurately mill a microchannel from the side of a PCF, to open selected holes in the cladding region.

In this paper, a versatile, robust, and integrated technique for selective filling is demonstrated by milling a microchannel into the end facet of a PCF. The PCF is then spliced to an SMF afterwards, so that only the desired air holes are exposed to the atmosphere for the following fluid infiltration. With this technique, it is possible to selectively fill any pattern of air holes in the PCF to achieve desired optical properties. Furthermore, since the splicing process is performed before the material infiltration, not only the aforementioned contamination problem can be avoided, but also a robust in-line device with improved integration and low coupling loss can be achieved, which is critical for most optical fiber applications and will be specially desirable for future gas filling fiber laser technologies.

2. Experiments

2.1 Fabrication Method

As shown in Fig. 1(a), the fabrication starts with a photonic crystal fiber (PCF, LMA-10, hole diameter 3 μm, interhole distance 6.6 μm, NKT Photonics A/S). A Helios EBS3 FIB with Ga^+ ion source is used here to mill microchannels for the lateral access in the following liquid infiltration. FIB has been used in a number of fiber-based applications, including fabrication of a Fabry-Pérot microcavity [11] and long period gratings [12], micromachining of fiber tips [13], and the milling of side access holes in structured optical fibers [10]. As a consequence of its applications in semiconductor technology, the FIB technique is mature and more flexible than the femtosecond laser processing, and dual-beam instruments combining a scanning electron microscope (SEM) and FIB are commercially available nowadays. The use of FIB as a milling tool allows quick and direct patterning via an ion bombardment process. During the milling process, there are excess charges cumulated on the surface of the material. These charges will cause random deflection of the incident ion beam and thus damage the milling profile. To avoid the charging effect, the fiber is fixed on top of conductive carbon tape attached to the grounded sample holder. Moreover, a thin layer of gold (about 5 nm) is deposited on to the end facet of the fiber surface to dissipate the excess electric charge. As shown in Fig. 1(b), rectangular patterns are defined on the end facet of the PCF to cover the desired air holes. The FIB milling is performed with an acceleration voltage and current of 30 kV and 20 nA, respectively. This high ion current leads to a fast milling speed and the whole

#152186 - $15.00 USD Received 1 Aug 2011; accepted 18 Aug 2011; published 22 Aug 2011

milling process duration is about 15 minutes to fabricate microchannels with a depth of ~5 μm.

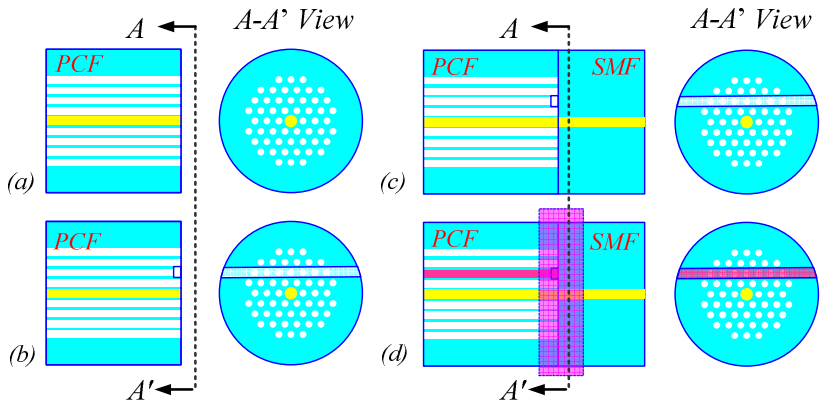

Fig. 1. Process flow for the selective filling of PCF. (a) A PCF is coated with a thin layer of metal on the end facet; (b) FIB is used to mill microchannels into the end facet of the PCF; (c) The PCF is then spliced to an SMF; (d) The sample is immersed in a fluid for infiltration.

The PCF (unfilled) is then spliced to an SMF with a fusion splicer, as shown in Fig. 1(c). The arc time and the current are adjusted to avoid that the air holes of the PCF and the milled microchannels collapse and to ensure a low splicing loss between the two fibers. We find that with an arc time of 0.2 seconds and an arc current of 10 A, the spliced SMF can successfully block all the undesired air holes and we can get a splice loss of only 1 dB.

As shown in Fig. 1(d), the fiber is finally immersed into a fluid, which then flows into the desired air holes through the lateral microchannel due to capillary action. In this way, selective filling of the PCF is successfully achieved.

2.2 Fabricated Sample

The proposed method is versatile and allows infiltration of any desired pattern of air holes. Here we demonstrate two configurations referred to as the central-line sample and the side-line sample, respectively. For the central-line sample, the air holes across the diameter of the end facet are selected and filled with liquid. For the side-line sample, one row of air holes off the diameter are selected and filled. Figure 2 shows SEM images for the two fiber samples after the FIB milling process. Figure 2(a) shows how the microchannel is milled across the air holes along the diameter of the end facet, while the central core is kept intact. A shallow microchannel is also milled offset one row for the following splicing test. Figure 2(b) shows a close-up view of the microchannels and the central core. From the side-view in Fig. 2(c), we can clearly see that the central line channel is milled about 5 μm deep while the shallow test channel is about 0.5 μm deep. The side-line sample is shown in Fig. 2(d). The microchannel is milled one row off the diameter with a rectangular pattern of 7 μm × 120 μm. In principle, lateral microchannels for any specific set of holes can be patterned with careful definition of the FIB milling strategy.

#152186 - $15.00 USD
Received 1 Aug 2011; accepted 18 Aug 2011; published 22 Aug 2011

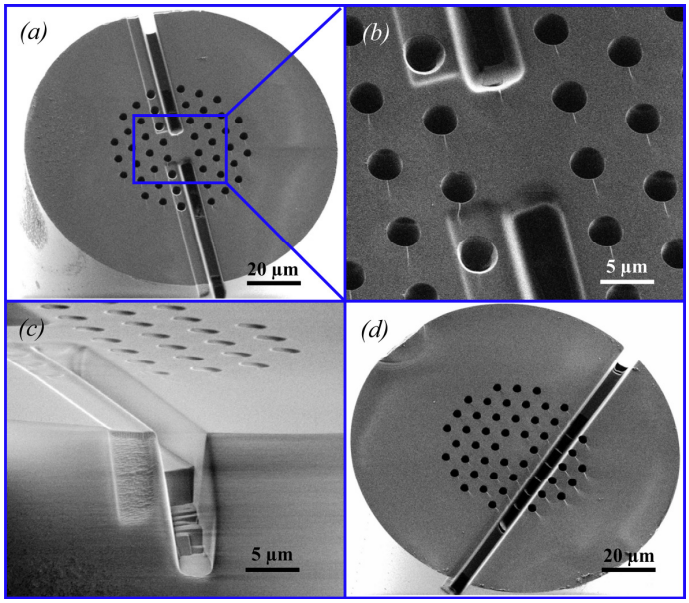

Fig. 2. (a) SEM image of the milled microchannels (~5 µm deep and ~5 µm wide, with a 0.5 µm deep channel next to it) across the central air holes on the end facet of PCF, (b) close-up top-view and (c) side-view of the microchannel across the central air holes. (d) A microchannel ~5 µm deep and ~7 µm wide across a side-line of air holes on the PCF end facet.

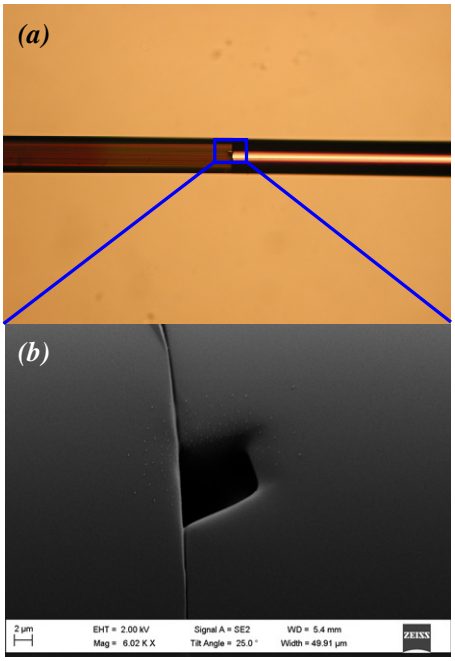

Fig. 3. (a) Microscope image of the spliced side-line sample; (b) SEM close-up view of the side-opening of the microchannel providing access to the desired air holes inside the PCF.

Figure 3(a) shows a microscope image of the spliced side-line sample. The splicing interface is clearly seen. A zoom on the opening of the lateral microchannel is further shown in the SEM image in Fig. 3(b).

#152186 - $15.00 USD
Received 1 Aug 2011; accepted 18 Aug 2011; published 22 Aug 2011

2.3 Infiltration and Characterization

To investigate the tuning properties of the selectively infiltrated fiber samples, a 10 cm length of both the central-line and side-line samples are spliced to an SMF. Then the samples are infiltrated over a length of 5 cm by capillary forces with a fluid (Cargille Laboratories, refractive index liquid) that has a refractive index of 1.68 at 589.3 nm and 25°C, and a negative thermo-optic coefficient of dn/dT ≈-3.4 × 10^{-4}/°C. In-line tunable fiber devices are formed by splicing the other end of the fiber samples to an SMF after the infiltration.

Several infiltrated devices of both configurations were fabricated. To confirm that the infiltration was successful, two of them were cleaved near the splice. Figures 4 shows microscope images of the cleaved end facets, which confirm that the refractive index liquid is successfully filled into only the desired air holes. For the central-line sample in Fig. 4(a), we can also see that the shallow microchannel is not filled with the refractive index liquid, which suggests that the 0.5 μm deep channel is too shallow to survive the splicing.

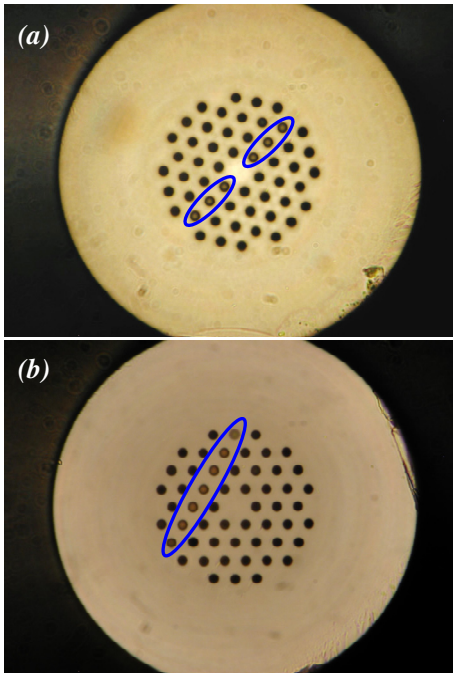

Fig. 4. Microscope images of the central-line sample (a) and side-line sample (b) after cleaving of selectively infiltrated PCFs close to the splice.

We now focus on the central-line sample in order to demonstrate that the final selectively filled device has the desired functionality, which is a hybrid fiber with bandgap guiding along one direction and total-internal reflection guiding along the orthogonal direction. Such a hybrid was first demonstrated in Ref [14]. A resistive hot stage (MC60 + TH60, Linkam) is used to gradually warm up the central-line sample from 25°C to 40°C. A superK Versa broadband source (NKT Photonics) is used to pump the fiber sample and an OSA (Ando, AQ6317B) is used to record the transmission spectrum. Figure 5 presents the transmission spectra of the central-line sample at different temperatures. The bandgaps within the spectrum from 1000 nm to 1750 nm indicate a hybrid fiber device formed. The Antiresonant Reflecting Optical Waveguide (ARROW) model predicts that the long wavelength edges of the bandgaps are given by $\lambda_m = 4d\sqrt{n_2^2 - n_1^2}/(2m+1)$ [15], where m is an integer; d = 3 μm is the hole diameter; n_2 is the isotropic refractive index of the liquid infiltrated into the air holes, and n_1 is the refractive index of silica. Assuming wavelength independent refractive indices of n_2 = 1.68 and n_1 = 1.45, we obtain the cut-off wavelengths λ_3 = 1454 nm and λ_4 = 1131 nm, which

#152186 - $15.00 USD Received 1 Aug 2011; accepted 18 Aug 2011; published 22 Aug 2011

are plotted in Fig. 5 with dashed lines. The predicted long-wavelength bandgap edges correspond nicely to the measured spectrum, in the 1000-1750 nm regime, thereby confirming the bandgap guiding mechanism. Estimated from the transmission 3 dB lower than the maximum (black horizontal dotted line in Fig. 5), the long-wavelength edge of the 2nd photonic bandgap shifts ~51 nm in response to the temperature increment of 15°C, which indicates a thermal tunability of ~3.4 nm/°C of the hybrid fiber device.

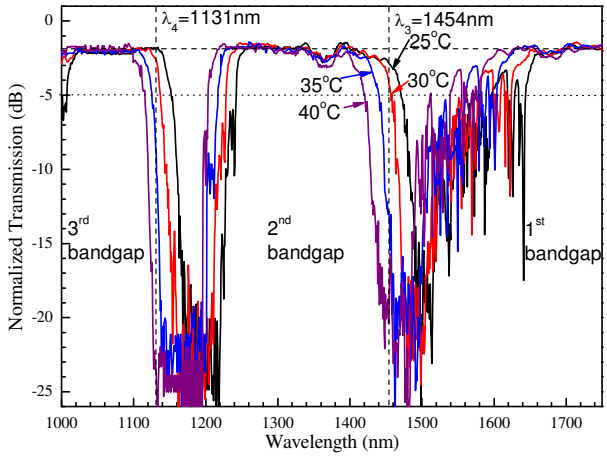

Fig. 5. Transmission spectra at 25°C (black), 30°C (red), 35°C (blue), and 40°C (purple) of the central-line sample infiltrated with 1.68-RI liquids.

To our knowledge, this is the first demonstration of a selectively infiltrated tunable hybrid fiber device and the resulting tunability is comparable with that of the previously reported liquid crystal infiltrated bandgap PCFs [16] and bandgap microstructured polymer optical fibers [2]. Obviously a higher thermal tunability could be achieved by using a fluid with a larger thermo-optic coefficient.

If we estimate the insertion loss from the peaks of the transmission spectra (horizontal dashed line in Fig. 5), which are normalized by the laser spectrum of the superK, we find that the insertion loss is about 2 dB. For our fiber device, the main origin of the insertion loss consists of two couplings between an index guiding mode and a hybrid guiding mode at the first splice and between the filled and unfilled sections of the PCF, one splice loss at the output and absorption loss of the liquid in the holes. In our case, the absorption loss is strongly reduced by only infiltrating one row of holes instead of all holes.

3. Conclusion

In conclusion, we have demonstrated a flexible and reliable method for selective infiltration of PCFs with the advanced FIB micromachining technique. With this method, it is possible to perform infiltration of arbitrary patterns of air holes via the side opening of a microchannel on the end facet of the PCF. In-line infiltration can be readily implemented with this method, which thereby enables highly efficient selective infiltration for the fabrication of novel fiber devices with low insertion loss.

Acknowledgments

The authors would like to thank Alexey Savenko from DTU Nanotech for help with the FIB milling at the Center for Electron Nanoscopy (DTU CEN). Center for Individual Nanoparticle Functionality, CINF, is sponsored by the Danish National Research Foundation.

#152186 - $15.00 USD Received 1 Aug 2011; accepted 18 Aug 2011; published 22 Aug 2011